Angewandte Chemie International Edition

DOI: 10.1002/anie.201208156

Porous Organic Cage Compounds

Post-Modification of the Interior of Porous Shape-Persistent Organic Cage Compounds**

*Markus W. Schneider, Iris M. Oppel, Alexandra Griffin, and Michael Mastalerz**

Cage compounds are fascinating molecules for several reasons.[1] They are defined molecular reaction vessels for "uncommon" products,[2] or used to stabilize highly reactive species in their interior.[3–5] Recently, materials made from purely organic cage compounds showed remarkable permanent porosities, with very high surface areas and good gas-sorption properties, both, in crystalline as well as amorphous phases.[6–8]

A feature that distinguishes the porous materials derived from cage compounds from those derived from extended network structures (such as metal organic frameworks (MOFs) and covalent organic frameworks (COFs)) is, that the intrinsically porous building units (the cage molecules) are soluble.[9] This creates several possibilities, which cannot be easily achieved for extended network structures or are even impossible. For instance, Cooper et al. reported on the co-crystallization of organic cage compounds in a binary or even ternary fashion to create porous organic alloys.[10,11] Very recently, this property was exploited to grow microporous cage crystals in mesoporous silica.[12] Another example of "processable" porosity has been demonstrated by our group:[13] various cage compounds, which are highly porous in the bulk, can be deposited as thin films on quartz crystal microbalances (QMBs) by spray-coating. The modified QMBs showed very good affinities for several aromatic analytes.

In 2008, we introduced the one-pot synthesis of the *endo*-functionalized [4+6] cage compound **3** by reacting four molecules of triamine **1** and six molecules of salicyldialdehyde **2** (Scheme 1).[14] What distinguishes this type of cage compounds from others, is that it bears six hydroxy groups pointing to the center of the cage cavity. This structural motif is very rare for organic cage compounds, and the functionalization of the cages interiors through reaction at the hydroxy groups was to date unsuccessful. Herein we present a facile method for the post-synthetic modification of the intrinsic voids in the cage compound, which allows the pore structure of the resulting material to be "fine-tuned" in the solid state.

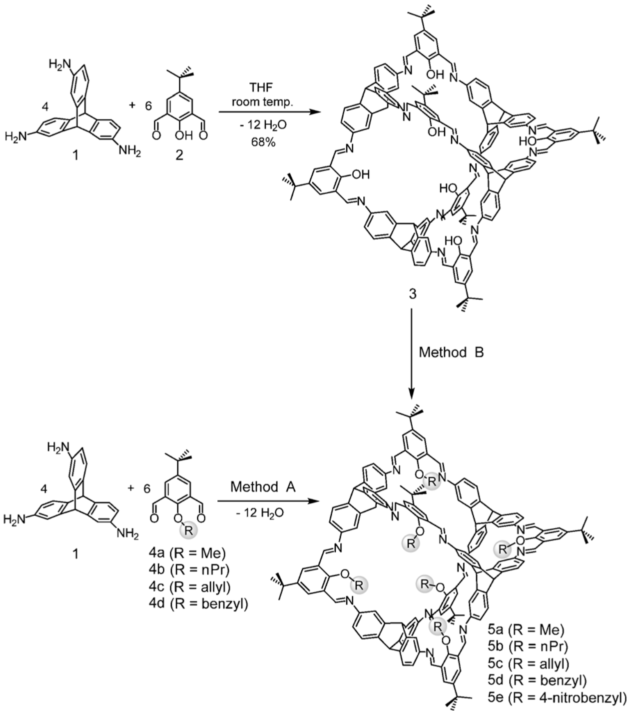

Scheme 1. Synthesis of cavity-modified cage compounds **5a–5e** by two different approaches. Method A: direct route by 12-fold imine condensation. Method B: Post-synthetically modification by sixfold Williamson ether formation. For reaction conditions, results, and yields, see Table 1 and Supporting Information.

Initially, we attempted to directly synthesize **5a** by the reaction of *O*-methylated salicyldialdehyde **4a** with triamine **1** (Method A in Scheme 1).[14] Unfortunately, only a small amount of cage **5a** was detected in the crude product by the MALDI-TOF mass spectroscopy.[14] However, cage **5a** could not be isolated by chromatographic methods.[15] Further optimization of the reaction conditions did not offer a decent route to synthesize **5a** in reasonable yield (never exceeding 17%). ^{1}H NMR analysis of the crude product (Figure 1b) exemplifies the high complexity of the resulting mixture. Similarly, reactions of triamine **1** with other salicyldialdehyde ethers **4b–4d** failed too. These unsuccessful experiments forced us to switch to an indirect approach (see

---

[*] Dipl.-Chem. M. W. Schneider, Dr. M. Mastalerz
Ulm University
Institute of Organic Chemistry II & Advanced Materials
Albert-Einstein-Allee 11, 89081 Ulm (Germany)
E-mail: michael.mastalerz@uni-ulm.de
Prof. Dr. I. M. Oppel
Inorganic Chemistry Department, RWTH Aachen
Landoltweg 1, 52056 Aachen (Germany)
Dr. A. Griffin
Oxford Diffraction (Agilent Technologies) Yarnton (UK)

[**] We thank the German Research Foundation (Deutsche Forschungsgemeinschaft) for funding (project MA4061/5-1) and the "Fonds der Chemischen Industrie" for the generous financial support. We thank C. Egger (Ulm University) for measuring the nitrogen sorption isotherms, and S. Blessing (Ulm University) for recording the PXRD data.

Supporting information for this article is available on the WWW under http://dx.doi.org/10.1002/anie.201208156.

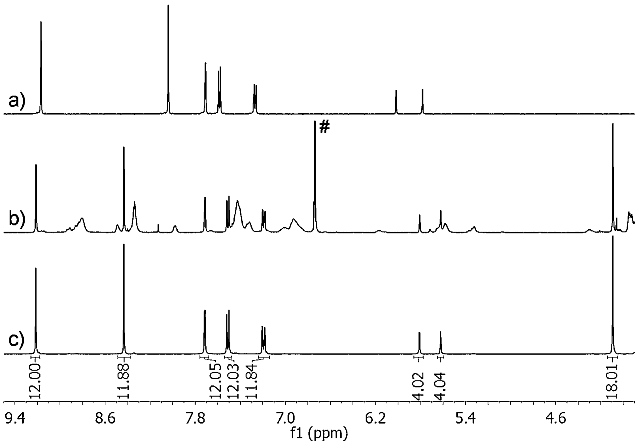

Figure 1. Partial ^1H NMR spectra of a) cage compound **3**, measured in [D$_6$]DMSO at 373 K; b) crude product of the reaction of **4a** and **1** (Method A); the # indicates aromatic protons of mesitylene, which was added as internal standard to quantify the amount of cage compound **5a** formed. c) Pure cage compound **5a** (Method B). b) and c) were measured in [D$_8$]THF. For full spectra and peak assignment, see Supporting Information.

Method B in Scheme 1): modifying the cage interior by introducing substituents after the cage scaffold is formed.

We started the investigation with methyl-group introduction by a six-fold Williamson ether synthesis. After optimizing the reaction conditions (1.2 equiv. MeI, DMF, K_2CO_3, 70 °C, 16 h), we were able to isolate **5a** in 82 % yield. The ^1H NMR spectrum of pure **5a** (see Figure 1 c) clearly shows a full conversion of all six hydroxy groups by a characteristic signal of the methoxy-group protons, resonating at $\delta = 4.09$ ppm with an integral of 18 H. The compounds purity and integrity was further confirmed by mass spectrometry, IR-, and ^{13}C NMR-spectroscopy, elemental analysis (see Supporting Information), and ultimately, single-crystal X-ray diffraction (see below).

To explore the scope of the post-synthetic modification by Williamson etherification, several alkyl halides were tested in the reaction (see Scheme 1, Table 1). However, we found that DMSO is a better solvent than DMF for reactions with all the other alkyl halide reagents. With this method we were able to introduce propyl (**5b**), allyl (**5c**), and benzyl (**5d**) substituents in high yields of 63 to 81 % (see Supporting Information). However, by using 4-nitrobenzyl bromide, only 12 % yield of **5e** was isolated, most probably because of the products low stability.

Table 1: Yields and specific surface areas of post-synthetically modified cage compounds **5a**–**5e**.

Compound	Yield[a] method A [%]	Yield[b] method B [%]	SA_{BET}[c] [$m^2\,g^{-1}$]	V_{pore}[d] [$cm^3\,g^{-1}$]
5a^{am}	17	81	824	0.43
5a^{cr}(200)[e]	–	–	741	0.38
5a^{cr}(rt)[f]	–	–	1700	0.71
5b	24	63	494	–[g]
5c	23	76	333	–[g]
5d	38	81	119	–[g]
5e[h]	–[g]	12	–[g]	–[g]

[a] Determined by integration of characteristic peaks in the ^1H NMR spectrum of the crude product against mesitylene as internal standard. [b] Yield of isolated product. [c] BET surface area determined by nitrogen sorption at 77 K. [d] Determined by NLDFT. [e] Activated at 200 °C [f] Activated at room temperature. [g] Not determined. [h] Compound decomposes within a few hours.

Cage compounds **5a**–**5d** were investigated by nitrogen sorption at 77 K to examine the impact of the introduced moieties on the specific surface areas determined by the Brunauer-Emmett-Teller (BET) model. All samples were degassed at 200 °C and 6×10^{-2} mbar for 3 h, prior to the measurement. As expected, with increasing bulkiness of the introduced moieties, the specific surface area decreases. For instance, the propylated cage **5b** gave a lower BET surface area (491 $m^2\,g^{-1}$) than the methylated cage **5a** (824 $m^2\,g^{-1}$). The allylated cage **5c** showed a slightly lower specific surface (333 $m^2\,g^{-1}$) than **5b**. If the bulky benzyl substituent is introduced, almost all of the voids interior is "filled", which results in a BET surface area of 119 $m^2\,g^{-1}$. Investigating the materials after performing the gas sorption experiments by powder X-ray diffraction (PXRD) revealed that all the samples are mainly amorphous (Supporting Information). It was reported before that the permanent porosity of periphery substituted [4+6] cage compounds is strongly depending on the morphology,[7d,16] which encouraged us to obtain crystalline material of the post-synthetic modified cage compounds.

We grew suitable single-crystals of **5a** for X-ray diffraction analysis by slow evaporation of solvent from a concentrated THF solution (Figure 2, left). Six molecules of **5a** crystallized in the unit cell with trigonal space group *R*3.[17] Since some THF molecules located inside the crystal voids could not be refined satisfyingly, the electron-density of disordered solvent molecules (64 % of the unit cell) was removed with the SQUEEZE function to elucidate the structure.[18] All the hydroxy protons in **5a** have been substituted by methyl groups. In contrast to the crystal structure of **3**, this substitution led to a repulsion of the imine nitrogen lone pairs and the oxygen lone pairs, which forces all the imine

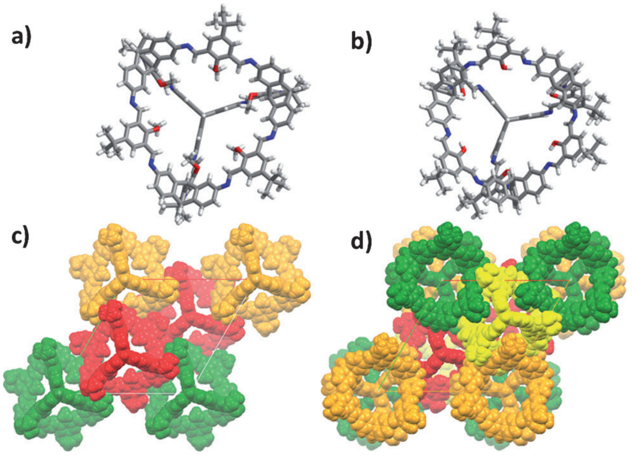

Figure 2. Single-crystal X-ray structures of **3** (right) and **5a** (left). a) and b) C_3-symmetric molecule. c) and d) packing. In (a) and (b): gray C, white H, blue N, red O. In (c) and (d) the molecules are colored to highlight the packing.

nitrogen atoms to change their orientation directing with their lone pairs out from the cavity, which remains shape-persistent. Most interestingly, there are some similarities to the crystal structure of **3**.[7d] First of all the molecular symmetry of C_3 is the same and the molecular dimensions are similar. The inner triptycene bridgehead protons build a slightly distorted tetrahedron with an average edge length of 11.4 Å (for **3** it is 10.4 Å). The six methyl carbon atoms form a distorted octahedron with an average edge length of 8.53 Å (The oxygen atoms form an octahedron with edge length of 9.70 Å). As mentioned, **5a** crystallized in the trigonal space group $R3$, whereas **3** crystallized in the trigonal space group $R\bar{3}$. However the dimensions of the unit cells are comparable. For **3** the length of the a and b axis is 29.15 Å, for **5a** it is 30.37 Å. Most interestingly, the packing of the molecules is very similar (see Figure 2c and d). In a very simplified way, removing the yellow as well as the upper green and orange highlighted molecules in Figure 2d, would give a similar pattern to that depicted in Figure 2c.

Consequently the unit cell of **3** contains the double number of molecules as found for **5a** and the c axis (58.52 Å) is double the length as that for **5a** (25.85 Å).The calculated density of the framework after in silico removal of residual solvent molecules is at 0.55 $\mathrm{g\,cm^{-3}}$ exceptionally low for a solid compound, indicating that the material is potentially very porous.[19] For **3** the density is comparable, 0.51 $\mathrm{g\,cm^{-3}}$.

Crystalline compound **5a** was investigated by nitrogen sorption at 77 K. If crystalline **5a** was treated analogously to the as-synthesized **5a** (200 °C and 6×10^{-2} mbar for 3 h) before measuring the nitrogen sorption isotherms, no significant difference in isotherm shape or the resulting specific surface areas, micropore volumes, and pore-size distributions is found (see Figure 3 and Table 1). PXRD of the crystalline material after gas sorption clearly showed that it became amorphous, which explains the similar sorption data.

The loss of crystallinity during the desolvation of porous molecular crystals is often accompanied by the loss of porosity, especially for extrinsically porous crystals. Recently, we have demonstrated that this loss of porosity can be prevented by a complete exchange of solvents.[20] We applied this method to crystalline **5a** to desolvate the material at room temperature (to give **5a^{cr}(rt)**) and indeed, with 1700 $\mathrm{m^2\,g^{-1}}$, the specific BET surface area is nearly double that of the amorphous material. It is worth mentioning, that this value is higher than for as-synthesized cage compound **3** (1377 $\mathrm{m^2\,g^{-1}}$) but lower than for crystalline **3** (2071 $\mathrm{m^2\,g^{-1}}$) and consequently the second highest reported for intrinsically porous materials derived from organic molecules.[6] PXRD after the gas sorption measurement revealed that the sample remained crystalline. The pore-size distribution has now a sharp maximum at 10.3 Å, which is comparable to that of **3**.[7d]

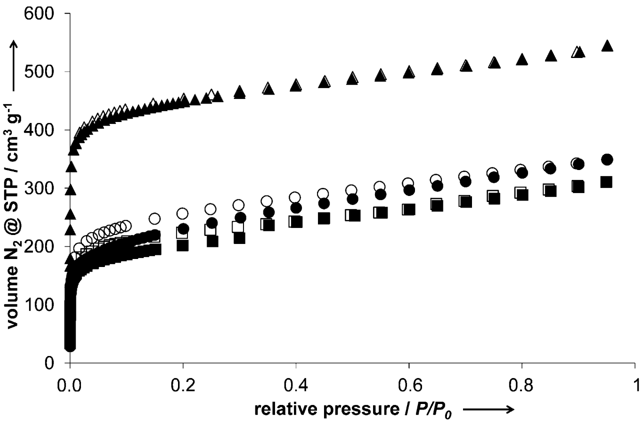

Figure 3. Nitrogen sorption isotherms of cage compound **5a** at 77 K. Closed symbols: adsorption; open symbols: desorption. Circles: amorphous material. Squares: crystals desolvated at 200 °C; triangles: crystals activated at room temperature after solvent exchange.

It is established that the adsorption of gas molecules is dominated by dispersion interactions, especially when the adsorbent is a covalent organic material.[21] Consequently, surface area and pore-size have a major effect for the adsorption of non-polar gases, such as methane. As expected, the curve progression for the heat of adsorptions of methane is very similar for both **3** and **5a^{cr}(rt)** with $\Delta H_{ads}(\mathbf{3})=40.7\ \mathrm{kJ\,mol^{-1}}$ and $\Delta H_{ads}(\mathbf{5a})=36.1\ \mathrm{kJ\,mol^{-1}}$ (Table 2). This suggests that only dispersion interactions are responsible and the material with the higher specific surface area (**3**, 2071 $\mathrm{m^2\,g^{-1}}$)[7d] shows a slightly better performance.

Table 2: Gas sorption data.

Compound	Adsorbed volume (wt%) at 1 bar [$\mathrm{cm^3\,g^{-1}}$]				ΔH_{ads} [$\mathrm{kJ\,mol^{-1}}$]	
	CO_2 273 K	CO_2 283 K	CH_4 263 K	CH_4 273 K	CO_2	CH_4
3	60.2 (11.8)	47.4 (9.3)	21.1 (1.5)	15.8 (1.1)	60.6[a]	40.7[c]
5a^{cr}(rt)	56.3 (11.0)	43.1 (8.4)	17.4 (1.2)	14.6 (1.0)	12.2[b]	36.1[d]

[a] At an adsorbed volume of 0.14 $\mathrm{cm^3\,g^{-1}}$. [b] At an adsorbed volume of 0.16 $\mathrm{cm^3\,g^{-1}}$. [c] At an adsorbed volume of 0.27 $\mathrm{cm^3\,g^{-1}}$. [d] At an adsorbed volume of 0.20 $\mathrm{cm^3\,g^{-1}}$.

However, the surface environment plays an additional role for the adsorption of polar gases. Since the pore surface of **3** with its hydroxy groups is more polar than that in **5a** with its methoxy groups, polarity might have a small but recognizable effect on the sorption of CO_2. Indeed, both compounds show very different heats of adsorption curves for CO_2 (see Supporting Information). For the more polar compound **3** the heat of adsorption at low adsorbed volume ($V=0.14\ \mathrm{cm^3\,g^{-1}}$) is very high ($\Delta H_{ads}=60\ \mathrm{kJ\,mol^{-1}}$) and with increasing adsorbed volume decreases to $\Delta H_{ads}=25\ \mathrm{kJ\,mol^{-1}}$ at $V=0.8\ \mathrm{cm^3\,g^{-1}}$, before leveling out between 25 and 27 $\mathrm{kJ\,mol^{-1}}$. For the less-polar compound **5a^{cr}(rt)**, the heat of adsorption at $V=0.16\ \mathrm{cm^3\,g^{-1}}$ is with $\Delta H_{ads}=12\ \mathrm{kJ\,mol^{-1}}$ significantly lower than for **3**. With increasing volumes, ΔH_{ads} reaches a level of approximately 22 $\mathrm{kJ\,mol^{-1}}$.

We assume that for the adsorption of CO_2 by **3** at low adsorbed volume, an additional interaction of the hydroxy moieties with the CO_2 molecules can occur through hydrogen bonding,[22] which would explain the high ΔH_{ads} value of

60 kJ mol^{-1} at low surface coverage. In contrast, for compound **5a$^{\mathrm{cr}}$(rt)**, there is no possibility for such hydrogen bonds, which is reflected in the small initial value for ΔH_{ads} of 12 kJ mol^{-1}. These examples clearly show that by the method presented herein the pores cannot only be adjusted in terms of specific surface area and pore volume but also in terms of function.

In summary, we have shown for the first time that the interiors of porous organic cage compounds can be post-synthetically modified in high yields. The numerous reaction sites can be transformed quantitatively, which greatly simplifies the purification procedure. This method provides a rapid way to enrich the organic-cage-compound family and opens opportunities, for example, to form porous organic alloys with versatile functionality.[11] It is worth mentioning that the post-synthetic functionalization of extended non-soluble porous frameworks by the formation of covalent bonds still is a difficult task.[23,24] In contrast to our approach, in most cases conversion of the interior functional groups is incomplete and very seldom surpasses 90 %.[25] Once more, this clearly underlines the advantage of solubility, which is an inherent property of porous materials derived from discrete organic molecules.

Received: October 10, 2012
Revised: December 19, 2012

Keywords: cage compounds · gas sorption · porous materials · post-synthetic modification · supramolecular chemistry

---

[1] For recent Reviews on supramolecular coordination cages, see: a) R. Chakrabarty, P. S. Mukherjee, P. J. Stang, *Chem. Rev.* **2011**, *111*, 6810–6918; For Reviews on organic cage compounds, see: b) M. Mastalerz, *Angew. Chem.* **2010**, *122*, 5164–5175; *Angew. Chem. Int. Ed.* **2010**, *49*, 5042–5053; c) N. M. Rue, J. Sun, R. Warmuth, *Isr. J. Chem.* **2011**, *51*, 743–768.

[2] a) M. Yoshizawa, J. K. Klosterman, M. Fujita, *Angew. Chem.* **2009**, *121*, 3470–3490; *Angew. Chem. Int. Ed.* **2009**, *48*, 3418–3438; b) B. Breiner, J. K. Clegg, J. R. Nitschke, *Chem. Sci.* **2011**, *2*, 51–56; c) D. Fiedler, D. H. Leung, R. G. Bergman, K. N. Raymond, *Acc. Chem. Res.* **2005**, *38*, 349–3358.

[3] D. J. Cram, M. E. Tanner, R. Thomas, *Angew. Chem.* **1991**, *103*, 1048–1051; *Angew. Chem. Int. Ed. Engl.* **1991**, *30*, 1024–1027.

[4] Z. Lin, J. Sun, B. Efremovska, R. Warmuth, *Chem. Eur. J.* **2012**, *18*, 12864–12872.

[5] P. Mal, B. Breiner, K. Rissanen, J. R. Nitschke, *Science* **2009**, *324*, 1697–1699.

[6] For Reviews, see: a) M. Mastalerz, *Chem. Eur. J.* **2012**, *18*, 10082–10091; b) N. B. McKeown, *J. Mater. Chem.* **2010**, *20*, 10588–10597; c) A. I. Cooper, *Angew. Chem.* **2011**, *123*, 1028–1030; *Angew. Chem. Int. Ed.* **2011**, *50*, 996–998; d) J. Tian, P. K. Thallapally, B. P. McGrail, *CrystEngComm* **2012**, *14*, 1909–1919.

[7] Examples of crystalline porous materials from organic cage compounds with high specific surface areas: a) T. Tozawa, J. T. A. Jones, S. I. Swamy, S. Jiang, D. J. Adams, S. Shakespeare, R. Clowes, D. Bradshaw, T. Hasell, S. Y. Chong, C. Tang, S. Thompson, J. Parker, A. Trewin, J. Bacsa, A. M. Z. Slawin, A. Steiner, A. I. Cooper, *Nat. Mater.* **2009**, *8*, 973–979; b) M. W. Schneider, I. M. Oppel, M. Mastalerz, *Chem. Eur. J.* **2012**, *18*, 4156–4160; c) M. Mastalerz, M. W. Schneider, I. M. Oppel, O. Presly, *Angew. Chem.* **2011**, *123*, 1078–1083; *Angew. Chem. Int. Ed.* **2011**, *50*, 1046–1051; d) M. W. Schneider, I. M. Oppel, H. Ott, L. G. Lechner, H.-J. S. Hauswald, R. Stoll, M. Mastalerz, *Chem. Eur. J.* **2012**, *18*, 836–847; e) M. J. Boyds, M. E. Briggs, J. T. A. Jones, D. J. Adams, S. Y. Chong, M. Schmidtmann, A. I. Cooper, *J. Am. Chem. Soc.* **2011**, *133*, 16566–16571.

[8] Examples of amorphous porous materials from organic cage compounds with high specific surface areas: a) J. Tian, P. K. Thallapally, S. J. Dalgarno, P. B. McGrail, J. L. Atwood, *Angew. Chem.* **2009**, *121*, 5600–5603; *Angew. Chem. Int. Ed.* **2009**, *48*, 5492–5495; b) M. W. Schneider, H.-J. S. Hauswald, R. Stoll, M. Mastalerz, *Chem. Commun.* **2012**, *48*, 9861–9863.

[9] J. R. Holst, A. Trewin, A. I. Cooper, *Nat. Chem.* **2010**, *2*, 915–920.

[10] a) J. T. A. Jones, T. Hasell, X. Wu, J. Basca, K. E. Jelfs, M. Schmidtmann, S. Y. Chong, D. J. Adams, A. Trewin, F. Schiffman, F. Cora, B. Slater, A. Steiner, G. M. Day, A. I. Cooper, *Nature* **2011**, *474*, 367–371; b) T. Hasell, S. Y. Chong, K. E. Jelfs, D. J. Adams, A. I. Cooper, *J. Am. Chem. Soc.* **2012**, *134*, 588–598.

[11] T. Hasell, S. Y. Chong, M. Schmidtmann, D. J. Adams, A. I. Cooper, *Angew. Chem.* **2012**, *124*, 7266–7269; *Angew. Chem. Int. Ed.* **2012**, *51*, 7154–7157.

[12] T. Hasell, H. Zhang, A. I. Cooper, *Adv. Mater.* **2012**, *24*, 5732–5737.

[13] M. Brutschy, M. W. Schneider, M. Mastalerz, S. R. Waldvogel, *Adv. Mater.* **2012**, *24*, 6049–6052.

[14] M. Mastalerz, *Chem. Commun.* **2008**, 4756–4758.

[15] It has been reported, that a similar type of cage compound is even stable in boiling water: T. Hasell, M. Schmidtmann, C. A. Stone, M. W. Smith, A. I. Cooper, *Chem. Commun.* **2012**, *48*, 4689–4691. However, to date there are no reports of any cage compound based on imine formation being stable during column chromatography.

[16] M. W. Schneider, L. G. Lechner, M. Mastalerz, *J. Mater. Chem.* **2012**, *22*, 7113–7116.

[17] Data were collected on an Oxford Diffraction SuperNova Atlas Dual system with a (Cu) microfocus source and focusing multilayer mirror optics. The structure was solved by direct methods and refined by full-matrix least-squares using SHELXTL-97.[26] All non-hydrogen atoms were refined using anisotropic thermal parameters. X-ray data have been deposited at the Cambridge Crystallographic Data Centre (CCDC 904717 contains the supplementary crystallographic data for this paper. These data can be obtained free of charge from The Cambridge Crystallographic Data Centre via www.ccdc.cam.ac.uk/data_request/cif.) Crystal Data for **5a**: $T = 100(2)$ K, $C_{158}H_{140}N_{12}O_6$, $M_r = 2302.82$, trigonal space group $R3$, $a = b = 30.374(4)$, $c = 25.851(5)$ Å, $V = 20655(6)$ Å^3, $Z = 3$, $\rho = 0.55$ g cm^{-3}, $\mu = 0.264$ mm^{-1}, $3.77° < \Theta < 75.9°$, reflections collected/unique 26726/13922 [$R(\mathrm{int}) = 0.0424$], reflections observed/restrains/parameters 10838/1/537 GOF 0.960, final $R[I > 2\sigma(I)]$ $R1 = 0.0553$, $wR2$ (all data) = 0.1549, residual density 0.155 and −0.226 e A^{-3}.

[18] a) P. Van der Sluis, A. L. Spek, *Acta Crystallogr. Sect. A* **1990**, *46*, 194; b) A. L. Spek, *Acta Crystallogr. Sect. D* **2009**, *65*, 148.

[19] K. J. Msayib, D. Book, P. M. Budd, N. Chaukura, K. D. M. Harris, M. Helliwell, S. Tedds, A. Walton, J. E. Warren, M. Xu, N. B. McKeown, *Angew. Chem.* **2009**, *121*, 3323–3327; *Angew. Chem. Int. Ed.* **2009**, *48*, 3273–3277.

[20] M. Mastalerz, I. M. Oppel, *Angew. Chem.* **2012**, *124*, 5345–5348; *Angew. Chem. Int. Ed.* **2012**, *51*, 5252–5255.

[21] R. T. Yang, *Adsorbents—Fundamentals and Applications*, Wiley, Hoboken, **2003**.

[22] A. Fujii, T. Ebata, N. Mikami, *J. Phys. Chem. A* **2002**, *106*, 10124–10129.

[23] S. M. Cohen, *Chem. Rev.* **2012**, *112*, 970–1000.

[24] for an example of a post-synthetic modification of a conjugated microporous polymer, see: B. Kiskan, J. Weber, *ACS Macro Lett.* **2012**, *1*, 37 – 40.

[25] for rare examples with conversion over 90%: a) K. K. Tanabe, Z. Wang, S. Cohen, *J. Am. Chem. Soc.* **2008**, *130*, 8508 – 8517; b) Y. Yoo, V. Varela-Guerrero, H.-K. Jeong, *Langmuir* **2011**, *27*, 2652 – 2657; c) M. Savonnet, D. Bazer-Bachi, N. Bats, J. Perez-Pellitero, E. Jeanneau, V. Lecocq, C. Pinel, D. Farruseng, *J. Am. Chem. Soc.* **2010**, *132*, 4518 – 4519.

[26] G. M. Sheldrick, SHELXTL-97, Universität Göttingen, Germany **1997**.

GDCh
GESELLSCHAFT DEUTSCHER CHEMIKER

IUPAC
International Union of
Pure and Applied Chemistry

IUPAC 2013
ISTANBUL

Travel grants for young chemists

IUPAC General Assembly and Congress

The 2013 IUPAC General assembly (August 8th -15th) and Congress (August 11th – 16th) will be held in Istanbul.

The German Chemical Society GDCh wants to encourage young chemists to participate in this unique Congress by offering six **travel grants**. Three for young chemists working in Germany and three for young chemists working in Eastern Europe. Each award consists of 1200 Euro as a contribution towards the travel costs and registration fees to attend the Congress.

The recipients are also expected to take part in the World Chemical Leadership Meeting, which is part of the General Assembly, to discuss their visions of the future of chemistry.

Applicants should be under the age of 35.

There is no specific application form, but applicants are required to provide: a letter of application, a brief CV, a confirmation of their current status and affiliation, a publication list, and a letter of support from the appropriate supervisor.

The deadline for receipt of applications is May 15, 2013.

Applications should be sent – preferably by email – to Barbara Köhler at the Gesellschaft Deutscher Chemiker (b.koehler@gdch.de)

© 2013 Wiley-VCH Verlag GmbH & Co. KGaA, Weinheim